AIAA-2005-4405

E×B Measurements of a 200 W Xenon Hall Thruster

J.M. Ekholm* and W.A. Hargus, Jr.†
Air Force Research Laboratory
Spacecraft Propulsion Branch
Edwards Air Force Base, California 93524

Abstract

Angularly resolved ion species fractions of Xe^{+1}, Xe^{+2}, and Xe^{+3} in the Busek BHT-200-X3 xenon Hall thruster plume were measured using an ExB probe for several operating conditions. The thruster was operated at nominal anode potential of 250 V and swept from 200 V to 325 V in 25 V increments. The ExB probe was placed 60 cm downstream of the exit plane and rotated up to 90° from centerline. At the nominal anode potential, the ion species fractions of the multiply charged xenon ions were lower, while at increased discharged voltages Xe^{+2} and Xe^{+3} showed an increase in their respective species fractions. At angles beyond 35°, an additional low energy peak was observed suggesting additional collisions in the far-field produce these low energy ions. Our goals are to characterize the thruster ion distribution and to verify predictions of various numerical models by investigating the effects of thruster operation and chamber backpressure on the production of charge exchange ions.

Nomenclature

$\vec{B}$ = Magnetic field
B = magnetic field strength [T]
d = distance between plates [m]
$\vec{E}$ = Electric field
E = electric field strength [V/m]
E_i = ion energy [eV]
e = elementary charge [C]
F = Lorentz force [N]
m_i = ion mass [kg]
q = charge
q_i = charge state of ion
$\vec{u}$ = ion velocity [m/s]
v_i = acceleration voltage [V]
V_p = probe voltage [V]
γ_i = secondary electron emission coefficient
ζ_i = ions species fraction

I. Introduction

The Hall thruster has been identified as a candidate technology for Earth orbit applications such as station keeping, orbit raising and transfers. Beforehand the physics behind the operation of the Hall thruster must be thoroughly understood. In particular, the interaction between the plume ions and spacecraft surfaces needs to be further characterized. Within the plume of the Hall thruster, multiply charged ions have been discovered along with Xe^{+1} [1]. High energy ions, such as doubly and triply charged xenon, have a potentially harmful effect on the spacecraft both in higher erosion and sputtering rates as well as decreased efficiency in the Hall thruster itself. The production and distribution of these ions, as well as their ion species fractions, need to be better understood. The goal of this work is to characterize the production and distribution of these high energy ions in the far-field of the plume where interactions with spacecraft surfaces may occur.

II. Apparatus

A. Function of the ExB Probe

In order to understand the formation and distribution of the multiply charged ions within the plume, the ions must first be separated according to their species and respective energy.

*Research Scientist, AFRL/PRSS, 1 Ara Road Edwards AFB, CA 93524, Member AIAA.
†Research Engineer, AFRL/PRSS, 1 Ara Road Edwards AFB, CA 93524, Senior Member AIAA.

Report Documentation Page

Form Approved
OMB No. 0704-0188

1. REPORT DATE	2. REPORT TYPE	3. DATES COVERED
MAY 2005		**-**

4. TITLE AND SUBTITLE	5a. CONTRACT NUMBER
ExB Measurements of a 200 W Xenon Hall Thruster	5b. GRANT NUMBER
	5c. PROGRAM ELEMENT NUMBER
6. AUTHOR(S)	5d. PROJECT NUMBER
J Ekholm; W Hargus, Jr.	**2308**
	5e. TASK NUMBER **0535**
	5f. WORK UNIT NUMBER
7. PERFORMING ORGANIZATION NAME(S) AND ADDRESS(ES)	8. PERFORMING ORGANIZATION REPORT NUMBER
Air Force Research Laboratory (AFMC),AFRL/PRSS,1 Ara Road,Edwards AFB,CA,93524-7013	
9. SPONSORING/MONITORING AGENCY NAME(S) AND ADDRESS(ES)	10. SPONSOR/MONITOR'S ACRONYM(S)
	11. SPONSOR/MONITOR'S REPORT NUMBER(S)

12. DISTRIBUTION/AVAILABILITY STATEMENT

Approved for public release; distribution unlimited

13. SUPPLEMENTARY NOTES

14. ABSTRACT

Angularly resolved ion species fractions of Xe+1, Xe+2, and Xe+3 in the Busek BHT-200-X3 xenon Hall thruster plume were measured using an ExB probe for several operating conditions. The thruster was operated at nominal anode potential of 250 V and swept from 200 V to 325 V in 25 V increments. The ExB probe was placed 60 cm downstream of the exit plane and rotated up to 90o from centerline. At the nominal anode potential, the ion species fractions of the multiply charged xenon ions were lower, while at increased discharged voltages Xe+2 and Xe+3 showed an increase in their respective species fractions. At angles beyond 35o, an additional low energy peak was observed suggesting additional collisions in the farfield produce these low energy ions. Our goals are to characterize the thruster ion distribution and to verify predictions of various numerical models by investigating the effects of thruster operation and chamber backpressure on the production of charge exchange ions.

15. SUBJECT TERMS

16. SECURITY CLASSIFICATION OF:			17. LIMITATION OF ABSTRACT	18. NUMBER OF PAGES	19a. NAME OF RESPONSIBLE PERSON
a. REPORT	b. ABSTRACT	c. THIS PAGE			
unclassified	**unclassified**	**unclassified**		**9**	

With schematics provided by NASA Glenn Research Center, an ExB probe was constructed for this purpose. Also known as the Wein Filter, the ExB probe acts as a velocity filter separating ions by their respective masses and charges, assuming all ions were accelerated through the same potential. Ions with differing charge states created within the discharge chamber will experience similar acceleration potentials resulting in vastly different velocities. The velocity of the various ions will be recorded as a function of the charge state.

As explained by Hofer and Kim [2-3], the ExB probe separates the charged particles through the use of the Lorentz Force equation.

$$F = qe(\vec{E} + \vec{u} \times \vec{B}) \tag{1}$$

This equation illustrates the deflecting force acting on a charged particle moving within electric and magnetic fields. Utilizing this fundamental aspect of nature, one can see by balancing the electric and magnetic fields a zero net force can be achieved.

$$0 = qe(\vec{E} + \vec{u} \times \vec{B}) \tag{2}$$

This allows the ions of a particular velocity to pass through the ExB region undeflected, relating the velocity of the charged particles to the electric and magnetic fields.

$$u = -E/B \tag{3}$$

Particles which successfully pass through the probe unhindered were recorded as current. The corresponding probe voltage is then related back to the energy of the ion which successfully traversed the ExB region [2].

$$E_i = q_i v_i = \frac{m_i}{2e}\left(\frac{V_P}{dB}\right)^2 \tag{4}$$

From the resulting velocity distribution function, the ratio of the ion species peaks, ζ_i, is determined, and the relationship between the ions species fractions expressed [3].

$$\Omega_i = \frac{q_i^{3/2}(1+\gamma_i)\zeta_i}{\sum_i \left(q_i^{3/2}(1+\gamma_i)\zeta_i\right)} \therefore \sum \zeta_i = 1 \tag{5}$$

B. Experimental Apparatus

The experiment was conducted in Chamber 6 located at the Air Force Research Laboratory (AFRL) Electric Propulsion Laboratory at Edwards AFB, CA. Chamber 6 measures 1.8 m diameter and 3.0 m length with a pumping speed of 32,000 l/s on xenon using four single stage cryopanels and one 50 cm dual stage cryopump. During operations chamber pressure is approximately 6×10^{-6} Torr, corrected for xenon.

The Busek Company BHT-200W-X3 Hall thruster, which is a primary propulsion system for microsatellites, was used in this experiment. The BHT-200 produces 12 mN of thrust at a system efficiency of 35% while operating at optimal discharge voltages and conditions. Table 1 shows the nominal operating conditions of the thruster used in this effort. During operation the magnet current was maintained at 0.75 A for increased stability due to the absence of plasma oscillations.

Table 1. Nominal Operating Conditions
Typical operating conditions of the Busek BHT-200-X3 Hall thruster.

Anode Flow	840 μg/s (Xe)
Cathode Flow	98 μg/s (Xe)
Anode Potential	250 V
Anode Current	0.85 A
Heater Current	3.0 A
Keeper Current	0.5 A
Magnet Current	0.75 A

The ExB probe consists of three main sections: the entrance collimator, ExB filter section, and exit collimator. The entrance collimator measures 88 mm in length with an entrance cap orifice of 1.6 mm. This section allows a narrow beam of charged particles to enter the ExB filter region. The ExB section measures 152.0 mm in length with apertures of 1.6 mm at each end. The exit collimator is 140 mm in length terminating at the tungsten coated ion collector.

Figure 1 depicts the ExB probe identifying the orientation of the electric and

magnetic fields. As moving ions enter the test section, they will be deflected by the Lorentz force, as seen by the path of the deflected ion, unless traveling at the desired velocity. Ions which transverse the ExB section unhindered exit through the output collimator and measured as current.

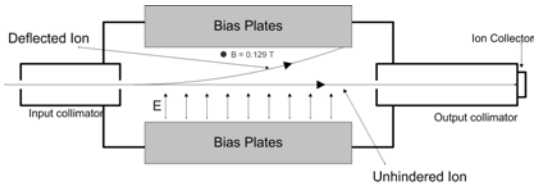

Figure 1. Electric and Magnetic Fields within the ExB Probe: *Path of unhindered and deflected ions transversing the ExB section.*

The magnetic field was supplied by two permanent magnets producing a field of 0.129 T, and a maximum flux of 0.163 T was measured in the center of the ExB region. For the purpose of analysis, the value of B in Eqn. 4 is taken to be the geometrical mean of the B field through the entire ExB test section. The electric field was created by applying a voltage to the two parallel bias plates.

$$E = \frac{V_p}{d} \tag{6}$$

The voltage between the two plates was swept from 0 to 60 V at 0.1 V increments, one plate ramped positive and the other negative using an Aglient 6614C voltage supply. Two 1 MΩ resistors were used to ensure a uniform potential was created between the two plates. With the magnitude of the magnetic field set at 0.129 T sweeping the current from 0 to 60 V is sufficient to deflect all ions with energy less than 1500 eV.

Ions passing unhindered through the probe were collected on a tungsten coated collector, and the resultant current measured on a Kiethley 6485 Picoammeter. All instruments, including the thruster and probe, were referenced to the chamber.

In order to rotate the thruster, the probe was placed on a stationary pedestal 60 cm from the BHT-200 and aligned with the nose cone using a laser, as seen in Fig. 2. Instead of rotating the probe around the thruster, the thruster assembly was rotated providing the ability to measure angles up to ±90° from centerline as seen in Fig. 3.

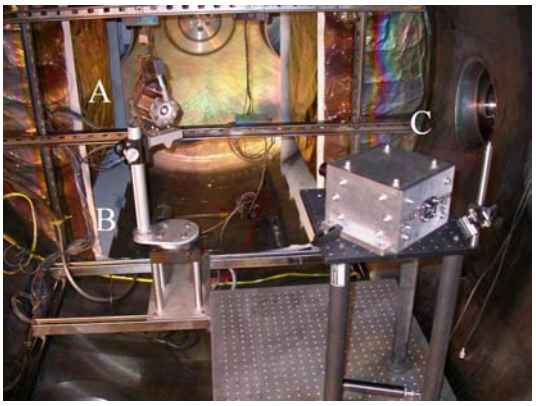

Figure 2: ExB Probe within chamber: *Note the ExB orientation to the thruster. A. BHT-200; B. rotation stage; C. ExB Probe - rear collimator has been removed.*

Special attention was given to the alignment of the thruster. The acceptance angle to the nose cone of the thruster was limited to ±0.5° and a distance of ±1 cm from the nose cone. Preliminary calculations into the uncertainty of the probe were performed as described by Kim [2]. Based on the dimensions and acceptance angles of both the entrance and exit collimator, the probe has a calculated uncertainty of ±4 eV.

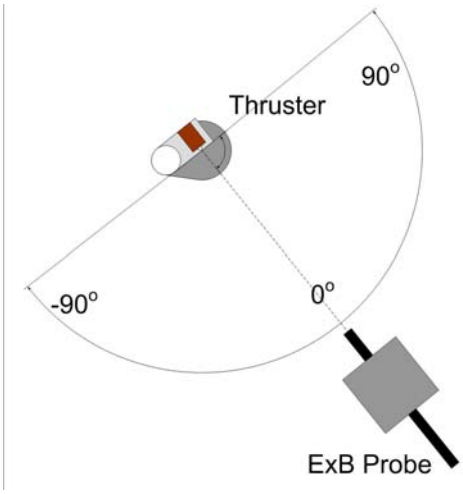

Figure 3: ExB and BHT-200 setup: *Rotation range of BHT-200. Centerline denotes thruster oriented directly at the probe.*

IV. Results and Analysis

A. Calibrations and Testing

Initial investigations in the plume showed the ExB probe well capable of distinguishing the respective Xe species. The thruster and probe were setup as previously discussed. At each of the operating conditions, the voltage applied to the bias plates swept from 0 to 60 V while the collector current was recorded. A range of 60 V was all that was necessary to clearly distinguish the various Xe signals as predicted, illustrated in Fig.4. Although a fourth, Xe^{+4}, peak was detected, its low magnitude had a negligible effect on the species fractions and will not be addressed further.

Signal broadening and over-lapping between the peaks was recorded, possibly due to collisions in the plume and within the ExB probe itself. Signal broadening is more apparent in the multiply charged species than Xe^{+1}, as seen in Figs. 5 and 6. The energy distribution seen in the peaks is attributed to charge exchange collisions by Kim [2]. These collisions inevitably affect the ion collection and measurement. With their velocities remaining unaffected, the ions are recorded at the same probe voltage, although accompanied with the slight deviation in measured current. To minimize the build of up pressure within the probe, several holes were bored in the rear plate. These holes assisted the flow through the probe preventing a build up of a localized high pressure zone within the ExB region, decreasing the likelihood of further collisions.

As seen in Figs. 4 and 5, signal broadening becomes apparent with Xe^{+3} with a full width at half maximum (FWHM) of 40 eV whereas Xe^{+1} has a FWHM of 20 eV in Fig. 5. In addition signal overlap between Xe^{+2} and Xe^{+3} raises concerns of glancing collisions between species within the plume as well as differentiation of the various species.

Initial measurements were made to calibrate the probe. While operating at 250 V, the trace, as seen in Fig. 4, was observed. The Xe^{+1} peak was recorded at 173.0 eV, corresponding to a velocity of 16,000 ± 500 m/s. This is in agreement with published values of Hargus and Charles' LIF, laser induced fluorescence, measurements of the same thruster [4].

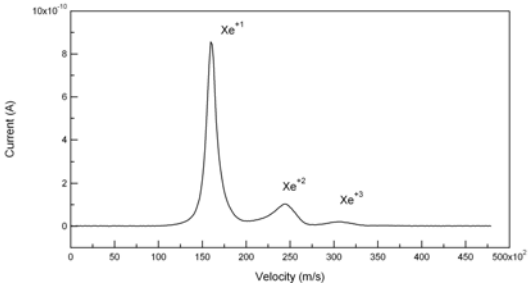

Figure 4. Velocity trace of 250 V ion species at -20 degrees: *Note the Xe^{+1} intense signal and detail. Xe^{+2} and Xe^{+3} begin to show decreasing intensity and signal broadening.*

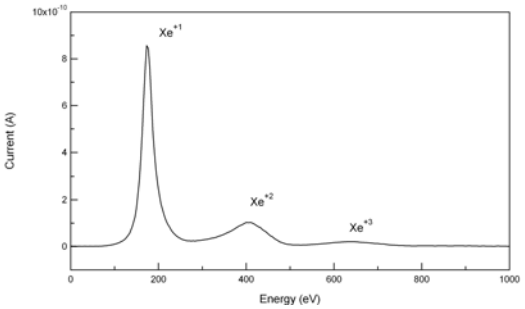

Figure 5: Energy trace of 250 V ion species at -20 degrees: *Note the sharp Xe^{+1} peak whereas Xe^{+2} and Xe^{+3} begin to show signal broadening.*

Table 2: 250 V Measurements: *Velocity and energy were recorded in agreement with Xe^{+1} Laser Induced Fluorescence measurements.*

Species	Energy (eV)	Velocity (m/s)
Xe^{+1}	173	16000
Xe^{+2}	405	24500
Xe^{+3}	632	30500

From the LIF data, Xe^{+1} had a velocity of 16,300 ± 500 m/s, well within the uncertainty. In addition to the uncertainty calculated through Kim's method, additional measurements were made using the LIF data. Through comparison, it is assumed the ExB probe has a velocity measurement uncertainty of approximately ±10%.

B. Angles Greater than 35°

Angles beyond 35° are of particular interest because charge exchange and spacecraft interactions are most likely to occur in this region. More specifically the distribution of multiply charged ions deserves a thorough analysis due to their higher energies and erosion rates on spacecraft surfaces. For this reason, the

ion species fractions in the far-field were also mapped.

At large angles plume interaction with the wall was feared. The thruster was mounted on a rotation stage and swept from 0° through 80°. Increased signal noise and significantly reduced signal beyond 80° placed measurements beneath the noise floor of the ExB probe and picoammeter. Some data was recorded at these angles, but noise obscured the actual current measurements from the collector making the peaks indistinguishable.

Several steps were taken to reduce signal noise and stabilize the baseline. Ram effect is a major concern with the quality of the data. With the probe oriented directly at the thruster, ions from the plume are entrapped within the probe creating a high pressure volume. Upon rotating the thruster to a new measurement position, a 10 minute pressure stabilization delay decreased the possibility of collisions within the probe. The delay of 10 minutes was adequate to allow the probe to equalize with the local flow. This step was performed with each iteration due to decreasing ion flux through the probe at increasing angles.

Secondly, 10 voltage sweeps of each angle were recorded and averaged creating a smooth and qualitative data set. The net effect of this procedure is to increase the signal to noise ratio by approximately 3x.

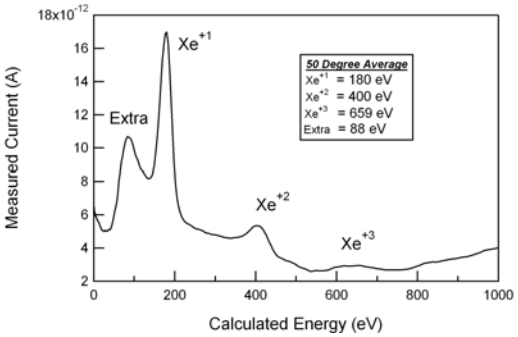

Figure 6: 50 Degrees: *All three ion species clearly visible.*

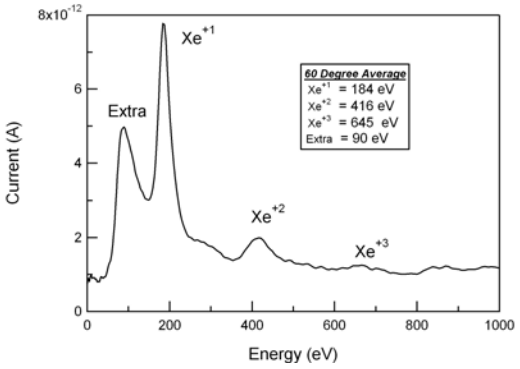

Figure 7: 60 Degrees: *All three ion species are visible yet Xe^{+3} is becoming unrecognizable in baseline.*

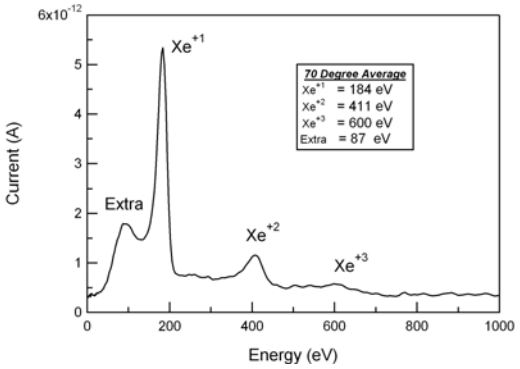

Figure 8: 70 Degrees: *Xe^{+1} and Xe^{+2} ion species are visible yet Xe^{+3} is nearly unrecognizable.*

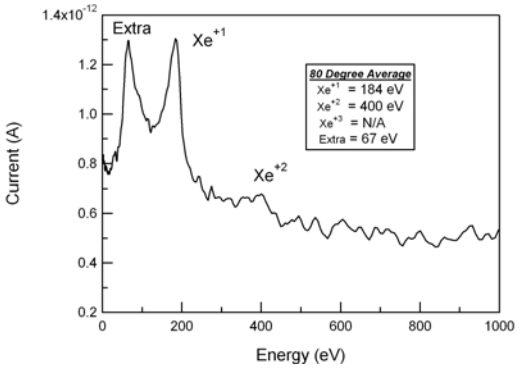

Figure 9: 80 Degrees: *Xe^{+1} is clearly visible while Xe^{+2} is nearly undistinguishable. Xe^{+3} is unrecognizable.*

Using the peak heights, the ion species fractions were determined using Hofer's method [3]. The results attained were in agreement with Hofer, Gallimore, and Kim [2-3, 6]. The ion species fractions in Fig. 10 show multiply

charged ion ratios increase as a function of the angle. In addition, Xe^{+1}, which continues to dominate the plume, experiences a decrease from 0.991 to 0.853 from 35° to 80° off centerline. Of particular interest is the region around 40° to 45°. In this region, Xe^{+1} experiences a sharp decrease within the plume while the multiply charged ions increase in population as seen in Fig. 10.

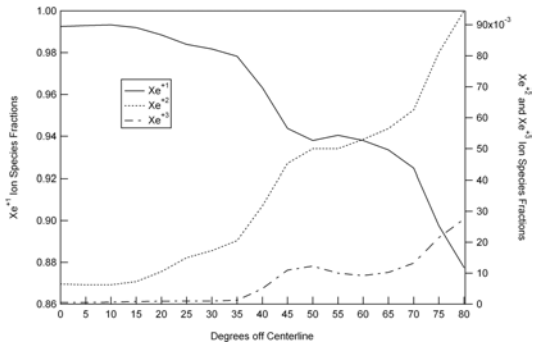

Figure 10: Ion Species Fractions in Far-Field: *Note the decrease of Xe^{+1} and the increase of multiply charged ions. Note sudden decrease at 45°. All measurements were taken at 5° increments.*

As seen in Fig. 6, 7, 8 and 9, an extra peak appears before the Xe^{+1} peak. This unidentified peak is also seen by King in the far field [5]. King relates these peaks to charge exchange collisions within the plume. Although, the energy associated with these ions (65 through 90 eV) is higher than expected. The peak emerges from the Xe^{+1} peak, becoming more distinguishable as the measurement angle increases as seen in Fig. 11, 12 and 13.

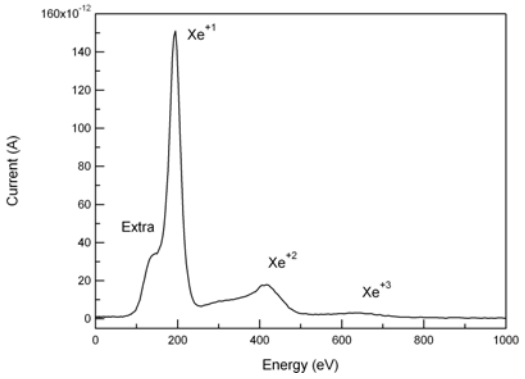

Figure 11: Emergence of Peak at 35 Degrees: *Unidentified peak begins to appear out of the Xe^{+1} trace.*

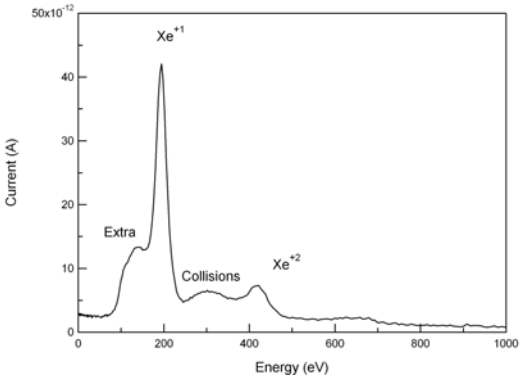

Figure 12: Emergence of Peak at 40 Degrees: *Unidentified peak becomes distinct, further separating itself from Xe^{+1} peak. Note the appearance of a rise in signal between Xe^{+1} and Xe^{+2} due to charge exchange.*

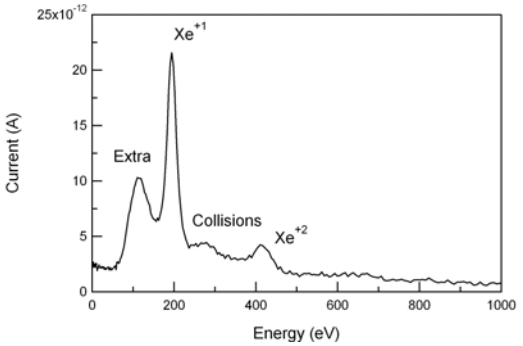

Figure 13: Emergence of Peak at 45 Degrees: *A possible low energy peak has begun to emerge. Again collisions are seen between Xe^{+1} and Xe^{+2}.*

The energy of the unidentified peak deceases as a function of the angle. Figure 14 shows the signal strength of the anomalous signal relative to the Xe^{+1} signal. Although the unidentified peak attains a maximum energy of 160 eV at 35° where it is first observed, the Xe^{+1} signal dominates until approximately 45°, at which their peaks attain nearly equal magnitudes. At more oblique angles the signals are comparable. A major drop in energy occurred at 45°, the same angle in which the peak became distinguishable from Xe^{+1}.

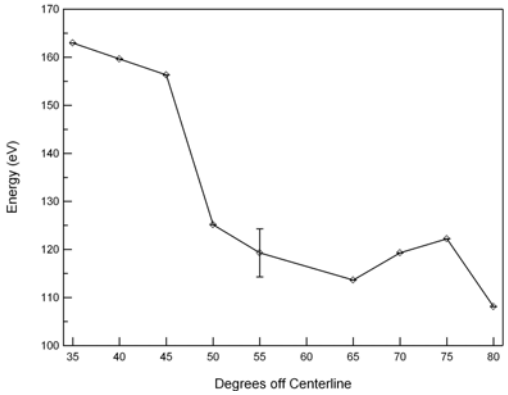

Figure 14: Additional Peak Energy: *The sudden decrease at 45^o. No data available at 60^0.*

Figure 15 compares the two peaks out to an angle of 80^o. At angles near 35^o, an order of magnitude separation between Xe^{+1} and the unidentified peak exists. However at angles beyond 50^o, both traces exhibit similar currents after a sharp decrease in Xe^{+1} magnitude.

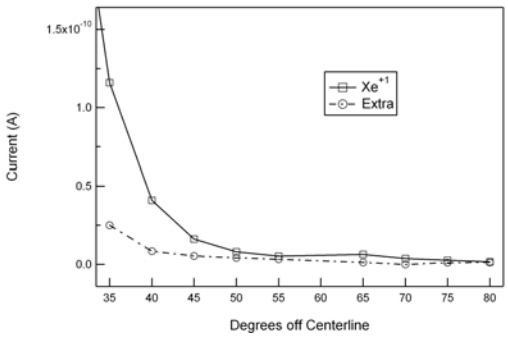

Figure 15: Xe^{+1} and Unidentified Line Intensity Comparison: *Initially Xe^{+1} signal dominates but by 45^o the unidentified peak has nearly attained equal magnitude.*

C. 200-325V Ion Species at Centerline

To uncover the effect of anode potential on the ion species fraction, the thruster anode potential was varied from 200 V to 325 V in 25 V increments. As expected, Fig. 16 shows a shift toward higher velocities across all three ion species corresponding to increasing anode potential.

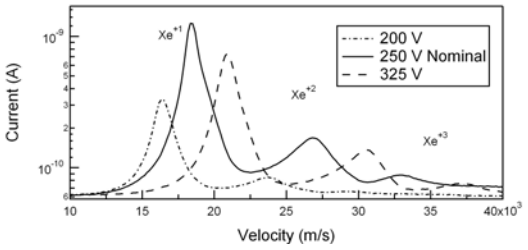

Figure 16. Effect of anode potential variance on the ion species fractions: *Note the increase in velocity as a function of an increase in anode potential.*

For the nominal 250 V anode potential, the singularly ionized xenon achieves a maximum of 0.955, whereas the doubly and triply charged xenon achieve fractions of 0.038 and 0.007 at the centerline. At the lower operating anode potentials, the multiply charged ions compose nearly 10% of the ion flow. As seen in Table 2, Xe^{+1} dominates over all anode potentials. As the anode potential increases to the optimal conditions, Xe^{+1} production increases as Xe^{+2} and Xe^{+3} production declines. It is interesting to note that the nominal condition represents a multiply charged ion minimum.

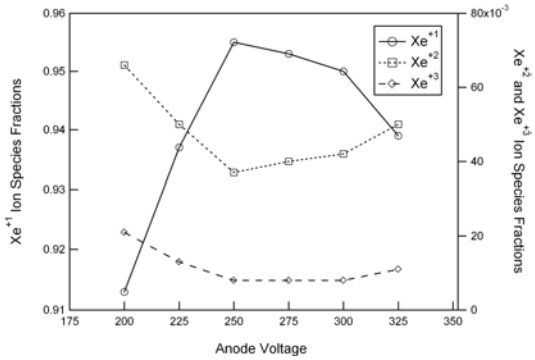

Figure 17: Respective Ion Species Comparison on Centerline of Thruster: *Note trends by all three species especially at nominal operating conditions of 250 V.*

Figure 17 shows a comparison of the species fractions as the anode potential is varied. The results indicate an increase in Xe^{+2} and Xe^{+3} at off-nominal operating potentials, while the Xe^{+1} fraction decreases. The data shows ion species fractions and multiply charged ion production is directly linked with anode potential.

Table 3: Ion Species Fractions of the BHT-200 measured at the centerline (60cm).

Anode (V)	Xe^{+1}	Xe^{+2}	Xe^{+3}
200	0.913	0.066	0.021
225	0.937	0.050	0.013
250	0.955	0.037	0.008
275	0.953	0.040	0.008
300	0.950	0.042	0.008
325	0.939	0.050	0.011

V. Conclusions

The ion species fractions of a BHT-200-X3 vary considerably throughout the plume. Anode potential and the angle from centerline have an effect on the species fractions and distribution of multiply charged ions.

In the far-field, ion species fractions show strong dependence on the angle. As expected signal strength decreases as ion flux in the far-field is greatly reduced. For this reason, measures were successfully taken to reduce noise and enhance the signal strength in the far-field. At the acute angles, Xe^{+1} dominated, but at angles greater than 45°, Xe^{+1} succumbed to increasing fractions of multiply charged ions. At 35° a separate unidentified peak emerges from the Xe^{+1} signal eventually becoming a distinct peak growing as a function of the angle. Although significant overlapping is apparent, the unidentified peak distinguished itself from the other species at 45°. Eventually the peak attains a signal comparable to Xe^{+1}. Many possible speculations as to the origin including elastic and charge exchange collisions can be made, yet its identification and origin remain unsolved.

The anode potential directly affects the fractions of all three ion species. Measurements indicate the Xe^{+1} species fraction is 0.955 at the nominal operating condition, 250 V, and then falls to 0.913 at an anode potential of 200 V. Whereas the multiply charged ions, Xe^{+2} and Xe^{+3}, species fractions remain lowest at the nominal operating condition and higher elsewhere.

Multiply charged ions in the far-field affect spacecraft Hall thruster integration. The high energy multiply charged ions are a source of increased erosion and sputtering on spacecraft surfaces. Understanding the source of these ions will facilitate the transition of Hall thruster to the spacecraft community.

VI. Future Work

Future research will be directed toward understanding the effects chamber backpressure and thruster operation conditions on ion plume species fractions at wide divergence angles between 35-90°. This work has only examined the far-field at one operating condition, and additional operating conditions will be needed to fully understand the ion species fractions in this region. The far-field properties will be examined at various anode potentials and compared to the centerline trends. In addition, the chamber backpressure will be increased possibly providing insight into the collisions causing signal broadening and distortion. In addition, the uncertainty inherent in the signal broadening will be further resolved, and the possibility of fringing fields within the probe will be resolved.

The unidentified peak needs to be better characterized. At only one operating condition its properties have only been slightly unveiled. Several differing operating conditions will be used to further determine its characteristics and origin.

New analysis techniques will be developed to measure ion species fractions. Resolution of signal broadening will provide insight into determining new methods of calculating the ion species fractions. Integrating the trace of each species will provide a more accurate measurement of the species fractions as opposed to peak height.

VII. Acknowledgements

Special thanks go out to Garrett Reed, and Michael Nakles of AFRL, and David Scharfe of Stanford University for assistance with the data acquisition software and initial stages of this effort. Also thanks goes to Richard Hofer from NASA Glenn Research Center for supplying the mechanical drawings for the ExB probes.

VIII. References

[1] D.H. Manzella, "Stationary Plasma Thruster Plume Emissions," IEPC-93-097, September 2003.

[2] S.W. Kim, "Experimental Investigations of Plasma Parameters and Species-Dependent Ion Energy Distribution in the Plasma Exhaust Plume of a Hall Thruster", University of Michigan, 1999.

[3] R.R. Hofer, and A.D. Gallimore, "Ion Species Fractions in the Far-Field Plume of a High–Specific Impulse Hall Thruster," AIAA-2003-5001, *39th Joint Propulsion Conference*, 20-23 July 2003, Huntsville, AL.

[4] W.A. Hargus, Jr. and C.S. Charles, "Near Exit Plane Velocity Field of a 200W Hall Thruster," AiAA-2003-5154, *39th Joint Propulsion Conference,* 27-29 July 2003, Huntsville, AL.

[5] L.B, King, "Transport-Property and Mass Spectral Measurements in the Plasma Exhaust Plume of a Hall-Effect Space Propulsion System," Dissertation, University of Michigan, May 1998.

6] S.W. Kim, and A.D. Gallimore, "Plume Study of A 1.35 kW SPT-100 Using An ExB Probe," AIAA-99-2423, *35th Joint Propulsion Conference*, 20-24 June 1999, Los Angeles, CA.